Photon-correlation detection of ion-oscillation frequencies in quadrupole ion traps

K. Dholakia, G. Zs. K. Horvath, D. M. Segal, R. C. Thompson,
D. M. Warrington,* and D. C. Wilson
Blackett Laboratory, Imperial College, Prince Consort Road, London, United Kingdom
(Received 23 June 1992)

We present a method for measuring ion-oscillation frequencies in quadrupole traps (Paul, Penning, and combined traps). The method depends on a statistical analysis of the delays between detected fluorescence photons. We have used the method to verify the oscillation frequencies for magnesium ions in a Penning trap as a function of the dc voltage applied to the trap electrodes. We demonstrate that, as expected, the method can measure the space-charge shifted (individual-ion) oscillation frequency rather than the frequency at which the ion cloud as a whole moves. However, our data suggest that for most of our operating conditions, any space-charge shift is negligible. We also discuss the effect of the contact potential arising from areas of the trap electrodes that are coated by excess Mg from the atomic beam used. We show that this extra potential shifts the center of the Penning trap and makes it unstable for low values of the applied voltage.

PACS number(s): 32.80.Pj

I. INTRODUCTION

The Paul, Penning, and combined traps share the same electrode structure which consists of two end caps and a ring (see Fig. 1) [1]. For the Paul trap, a large radio-frequency voltage V_{ac} is applied between the ring and end caps, setting up a three-dimensional pseudopotential well typically a few electron volts deep. For given values of Ω (the rf drive frequency) and the ionic mass (M), such a trap is only stable for a limited range of V_{ac}. The stability of the trap can be increased by applying, in addition to V_{ac}, a dc potential V_{dc} between the ring and end caps [2].

If V_{dc} is applied in the absence of V_{ac} a simple electrostatic quadrupole potential is set up near the center of the trap. At this point the potential has a saddle point (if the end caps are held positive with respect to the ring there is a minimum in the z direction and a potential hill in the radial plane). Radial confinement can be achieved by placing the trap in a strong magnetic field (B) which forces the ions into orbits in the xy plane (the Penning trap). An ion's radial trajectory in the Penning trap is an epicyclic superposition of two circular motions; a slow drift around the center of the trap at the magnetron frequency (ω_m) and a faster rotation at the modified cyclotron frequency (ω_c'). There is a single axial oscillation frequency (ω_z). For positive ions of mass M and charge e the relevant frequencies are given by [3]

$$\omega_c = \frac{eB}{M}, \tag{1}$$

$$\omega_z = \left[\frac{4eV_{dc}}{M(r_0^2+2z_0^2)}\right]^{1/2}, \tag{2}$$

$$\omega_m = \frac{\omega_c}{2} - \left(\frac{\omega_c^2}{4} - \frac{\omega_z^2}{2}\right)^{1/2}, \tag{3}$$

$$\omega_c' = \frac{\omega_c}{2} + \left(\frac{\omega_c^2}{4} - \frac{\omega_z^2}{2}\right)^{1/2}, \tag{4}$$

where ω_c is the cyclotron frequency and $2r_0$ and $2z_0$ are the diameter of the ring and separation of the end caps, respectively. Often r_0 and z_0 are combined to form a single parameter R through the expression $R^2 = 2z_0^2 + r_0^2$. For our trap $R^2 = 2r_0^2 = 4z_0^2$ and typical values for ω_m, ω_c', and ω_z are 50, 500, and 250 kHz, respectively.

To create a combined trap [2,4], all of the fields of the Paul and Penning traps are applied simultaneously. The equations of motion for ions in such a trap can be cast in the form of Mathieu equations which can be solved exactly yielding three oscillation frequencies [4] (ω_z and two radial frequencies for the two radial degrees of freedom).

Paul and Penning traps have been used widely for high-precision experiments on small numbers of, and even single, charged particles (e.g., ions, electrons, positrons) [5]. With strong laser cooling, ions in a Paul trap have been made to crystallize into rigid structures [6]. The number of ions that can be trapped in a Paul trap is limited by radio-frequency heating [7]. Larger clouds of ions can be held in a Penning trap and ions in such clouds have been observed to form into shell structures [8]. The combined trap is of considerable interest since it offers enlarged re-

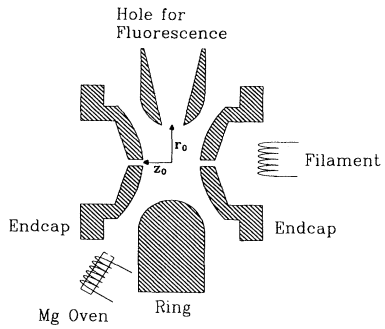

FIG. 1. Schematic diagram of the trap used in this work. The position of the Mg oven is shown.

gions of stability as a function of V_{ac} and V_{dc}, making it possible to trap oppositely charged particles of widely differing mass in the same trap at the same time [9].

It is often desirable to know the oscillation frequencies of ions confined in the various kinds of quadrupole trap. For Penning, Paul (rf), and combined traps these frequencies have often been measured by driving the ion cloud with a small additional oscillating voltage applied to the trap electrodes. This can be done while simultaneously laser cooling the cloud. The drive frequency is varied, and when a resonance is reached the ion cloud absorbs energy from the electrical drive. This leads to a change in the fluorescence signal from the ion cloud (sometimes the fluorescence increases and sometimes it decreases, depending on the laser detuning) [10]. It is also possible to keep the drive frequency fixed, varying another parameter such as the dc trapping potential, to bring the ions into resonance.

This method is time consuming and has a number of drawbacks. First, one cannot apply a voltage to the trapping electrodes which directly drives motion in the radial plane; in order to do this, either a split ring or other extra electrodes which break the cylindrical symmetry must be incorporated into the trap design. In a symmetric trap the radial motion is only indirectly driven by any weak coupling that may exist between the axial and radial motion, as a result of, for example, misalignment of the trap axis with respect to the magnetic field. Second, the method is invasive, in that the cloud is strongly perturbed by the application of the drive voltage. This may lead to some inaccuracy in the value for the frequency which is determined. Furthermore, the cloud is sometimes so strongly perturbed that it heats up and is lost from the trap. Third, the method can display hysteresis in that the measured value for the resonant frequency can depend on whether the drive frequency is scanned up or down. Another point worthy of note is that this method measures the center-of-mass frequency, i.e., the frequency at which the whole cloud moves in the trap. It does not measure the frequency at which individual ions move in the trap, which is altered by the presence of the other ions [3]. Whether this is considered as an advantage or a disadvantage naturally depends on the application.

In this paper we report a method for measuring ion-oscillation frequencies in traps and apply it to the case of magnesium ions in a Penning trap. Taking into account trap perturbations, we have verified the calculated values of the various trap resonances over a wide range of V_{dc}.

As the ions execute their orbits in the trap, the Doppler effect ensures that they move in frequency alternately closer to, and further from, resonance with the cooling laser. The ions may also move spatially in and out of the focused laser beam. The level of scattered light is therefore modulated at the oscillation frequency. Since the detection efficiency is usually such that less than one photon is detected per oscillation period, the modulation cannot be observed directly. It does, however, affect the statistics of the photon-count pulse train. By performing an appropriate statistical analysis of the photon-pulse arrival times, information about the oscillation frequencies can be retrieved. Our method has similarities with work conducted by Diedrich and Walther [11] and by Blümel *et al.* [7] in which the modulation of the fluorescence rate due to the micromotion and secular motion of Mg ions in a Paul trap was observed using photon-photon and photon-rf correlation methods. However, in our method we apply a statistical analysis which enables us to determine all the ion-oscillation frequencies in Penning, Paul, and combined traps.

II. EXPERIMENT

The trap and laser system used for this work have been described in detail in Ref. [4]. Briefly, the trap has an end-cap separation of $2z_0 = 7$ mm and an internal diameter of $2r_0 = 10$ mm. It is housed in an UHV vessel maintained at less than 3×10^{-10} mbar (see Fig. 1). The laser radiation required for cooling and detection is generated by frequency doubling the 650-mW cw output of a Rhodamine 110 ring dye laser running on a single mode at 560 nm. The frequency doubling is performed in a temperature-tuned deuterated ammonium dihydrogen phosphate (AD*P) crystal typically giving an output of ~ 75 μW of uv radiation at 280 nm. The 280-nm beam is passed through diametrically opposing holes drilled in the ring electrode, and is focused to a $\sim$ 50-μm-diam waist at the center of the trap. The fluorescence is detected through a third hole in the ring at 90° to the laser beam. Magnetic fields up to $B \sim 1$ T were provided by a conventional electromagnet and V_{ac} could be varied up to $\sim$ 230 V in amplitude. $\Omega/2\pi$ was set at 2.57 MHz, at the resonance of a tuned circuit. V_{dc} could be varied between -20 and $+20$ V.

The fluorescence is collected using a two-lens imaging system and is focused onto the photocathode of a low-dark-current photon-counting photomultiplier tube (PMT). The overall detection efficiency, which is affected primarily by the solid angle of detection and the PMT quantum efficiency, is approximately 1×10^{-3}. The PMT is connected to a discriminating amplifier producing emitter-coupled-logic (ECL) pulses which are then converted to transistor-transistor-logic (TTL) pulses of approximately 10-ns duration. For the signal levels used throughout our experiments [$<$ 50 000 counts per second (cps) and usually $\sim$ 5000 cps] the photon pulses are well separated in time. The TTL pulse train is fed into a time-to-amplitude converter (TAC). The TAC is started by the arrival of the first TTL pulse and stopped by the next one. An output voltage proportional to the measured delay Δt is generated and passed on to a multichannel analyzer (MCA) card housed in a personal computer (PC). We collect data for typically a few minutes, giving a total count of $\sim 10^6$. The full scale of the TAC can be set to a convenient value given that the total number of MCA bins is fixed at 2048. We routinely run with a full scale of 500 μs. For randomly arriving pulses the output of the MCA is an exponentially decaying function of Δt. When periodic modulation of the fluorescence is present, the output consists of peaks at multiples of the modulation period contained within an exponentially decaying envelope.

Our method differs from that used by Blümel *et al.* to produce Fig. 8 of Ref. [7] in that they derive their TAC start pulse from the signal generator producing the rf field. The TAC stop pulse is then given by the arrival of a photon (photon-rf correlation). This method cannot be used in a Penning trap where the rf field is absent. Our method has more in common with that of Diedrich and Walther (Ref. [11]) in which photon-photon correlations were observed. In that experiment two separate photomultipliers were used to generate the TAC start and stop pulses so that very short intervals, less than the photomultiplier dead time, could be investigated (in this way they were able to demonstrate photon antibunching; the micromotion showed up as a modulation of their correlation plot at relatively long times). Detection of the secular motion of ions in a Paul trap was also demonstrated in Figs. 12 and 13 of Ref. [7], using a correlation technique.

In a cloud of ions there exists a phase difference between the secular motion of a given ion and any other ion in the trap. This phase difference is, in general, unpredictable since it depends in a complicated way on the dynamical behavior of the ions; it may also vary with time. In the photon-photon correlation method, correlations only exist between consecutive photons emanating from the same ion. Consequently the method can only be applied to small clouds of ions. For larger clouds, the modulation of the correlation plot is washed out. It is worth noting that in a Paul or combined trap, the micromotion can be detected, using either photon-photon or photon-rf correlations, for arbitrarily large clouds since the rf drive imposes a uniform phase on the ion micromotion.

When taking data the MCA output is plotted and updated in real time on the computer screen. It is left to run until the peak structure appears well enough defined. We have found that ~200 s is usually sufficient. The data is then read into a program which performs a fast Fourier transform (FFT) on the MCA trace. In our method the inclusion of the Fourier transform is crucial. With up to four different oscillation frequencies affecting the light modulation, the associated correlation plot is often very complicated (see Fig. 2). If one or more of the frequencies to be measured only results in a weak modulation of the correlation plot it is impossible to measure the modulation period by inspection. Often the FFT reveals clear modulation frequencies which can only be discerned in the correlation plot with the benefit of hindsight, if at all.

The 500-μs MCA range was chosen to be compatible with the needs of the Fourier transform, whilst bearing other constraints in mind. The range is kept long so that as many peaks as possible can be sampled by the FFT even for the lowest frequencies to be measured. This gives a high spectral resolution in the FFT (2 kHz in our case). There are two practical upper limits to the MCA range. Firstly, the decay constant of the exponentially decaying function is set by the mean photon count rate in the experiment. Under normal operating conditions delays longer than 500 μs were rare, setting an upper bound on the MCA range. Secondly, to avoid aliasing in the Fourier transform, the MCA bin width should be smaller than half the period of the fastest modulation present in the MCA correlation plot. With a 500-μs range (0.25-μs bin width), this condition is clearly not met by the micromotion frequency of 2.57 MHz (0.39-μs period). However, since this frequency is fixed throughout the experiment, and since its alias can be easily calculated, we can tolerate its presence in our transforms.

The periodic modulation present in the MCA correlation plot is only expected to be cosinusoidal if the amplitude of the ionic motion is small. If the modulation present in this plot is not purely cosinusoidal, the resulting transform will contain the higher harmonics needed to synthesize the shape of the peaks. The appearance of higher harmonics in the Fourier transform does not therefore necessarily mean that oscillations at these frequencies are occurring in the trap (although the possibility that they may be present cannot be entirely discounted). Likewise, whilst sum and difference frequencies often appear in the transform, these frequencies are not interpreted as true oscillation frequencies. A typical MCA correlation plot and its Fourier transform, for the combined trap, are shown in Fig. 2.

Modulation at twice the magnetron frequency, rather than at the actual magnetron frequency, is frequently

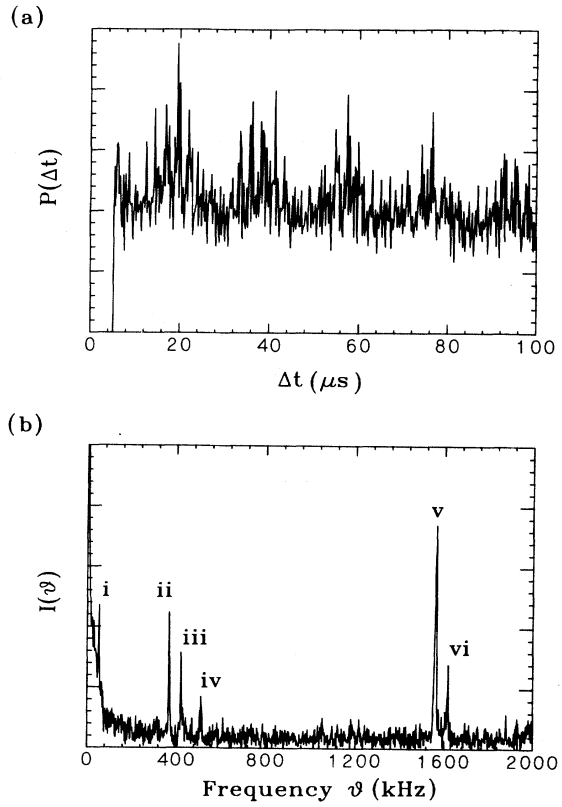

FIG. 2. A typical MCA correlation plot (a) and its Fourier transform (b) taken for a combined trap with V_{ac}=223 V and B = 0.55 T. The frequencies on the FFT correspond to (i) ν_{rl}; (ii) ν_{ru} ; (iii) $\nu_{rl} + \nu_{ru}$; (iv) ν_z ; (v) alias of $\Omega/2\pi$; and (vi) alias of $\Omega/2\pi + \nu_{rl}$. (ν_{rl} and ν_{ru} are the combined trap upper and lower radial frequencies [4].)

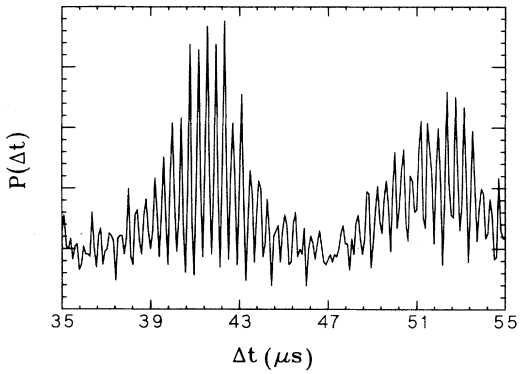

FIG. 3. MCA correlation plot for a single ion confined in a combined trap. The rapid oscillation is the rf drive and the slower modulation is the lower radial frequency (which correlates with the magnetron frequency in the Penning trap limit). For a single ion all the detected photons are correlated and so the modulation is deeper than for the case of an ion cloud.

observed. We attribute this to be due to the motion of the ion, which either takes it physically in and out of the focused laser beam, or in and out of resonance with the laser via the Doppler effect. Whether it is ν_m or $2\nu_m$ that is observed then depends on the position of the beam waist and upon the laser detuning from resonance. For example, if the beam passes nearly centrally through the trap, and the beam waist is smaller than the dimensions of the ion cloud, then a given ion will pass through the laser beam twice per oscillation period. On the other hand, if the laser is focused at the edge of the ion cloud then ions only pass through the beam waist once per oscillation cycle.

Figure 3 is a correlation plot for a single ion in a combined trap. The depth of modulation of the plot is much greater than for the case of an ion cloud, since, for the single ion, *all* the pairs of stop and start photon pulses are correlated.

Our specific interest in this method is in connection with the possible formation of small ion crystals, similar to those already seen in a Paul trap [6], in the Penning trap. Even if small numbers of ions do indeed form ordered structures in a Penning trap the individual ions could not be imaged as a result of their rotation in the laboratory frame [8]. However, the formation of an ordered structure in the trap should be accompanied by the appearance of new modulation frequencies for the fluorescent light. It may be that the spectrum of ion-oscillation frequencies can act as a signature of the kind of structure present in the trap.

III. RESULTS AND DISCUSSION

A. Space-charge shift

Since correlations only exist in general between consecutive photons emanating from the same ion, we would expect to observe the oscillation frequencies of individual ions within the cloud rather than some property of the ion cloud as a whole. This is in contrast to the usual method for measuring ion-oscillation frequencies in which the cloud is driven to oscillate as a whole in the trap. Since the cloud has the same charge-to-mass ratio as a single ion it is the single-ion frequency that is measured [3]. Figure 4 shows the Fourier transforms of three correlation plots taken in succession in a Penning trap. A small cloud of ions had just been loaded prior to the first data collection run. The peaks give the magnetron frequency. Note that, as the cloud cools under the influence of the laser, the magnetron frequency shifts from its calculated value to a higher frequency. This shift is in the right direction since the presence of other positive charges in the trap tends to steepen the radial potential hill responsible for the magnetron motion. The amount of shift allows us to calculate the ion density (n) and thus the average interion spacing (d) in the trap, giving $n = 1.0 \times 10^7$ cm^{-3} and d =46 μm for the conditions of the final trace in Fig. 4.

The peaks in Fig. 4 become weaker and more diffuse as the cloud becomes cooler. This is to be expected since, as the ions slow down, they become more confined to the center of the trap and spend more time in the laser beam,

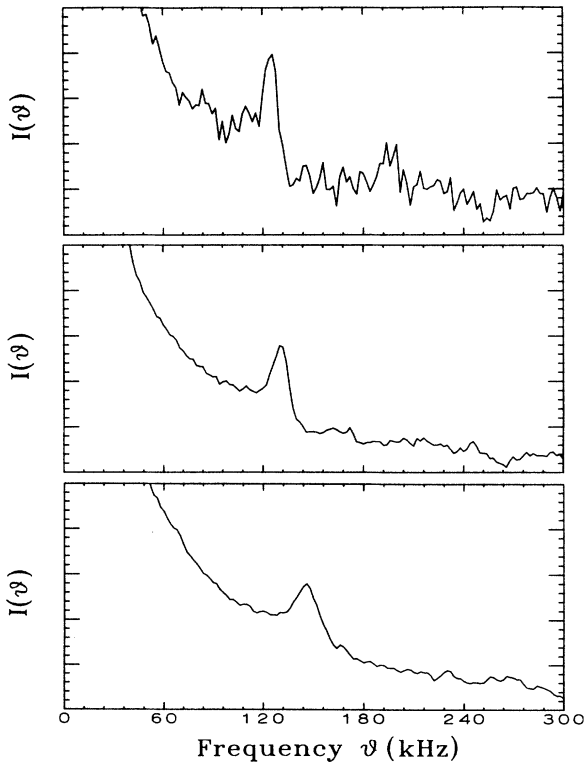

FIG. 4. Fourier transforms for three correlation plots taken consecutively in the Penning trap. The peak in each case occurs at 2× the magnetron frequency. As the ions cool down into the laser beam the photon count rate increases and the peaks shift to higher frequency. The magnetron frequency given by the first (top) trace agrees with the value calculated in the absence of space-charge shift.

reducing the modulation. The other source of modulation, the Doppler effect, is also reduced as the ions slow down. However, the peaks will also be broadened by the fact that the rotation frequency probably changed significantly during the finite time taken to record the correlation plot. This method represents a new way of measuring space-charge-shifted frequencies.

Other methods have been employed to measure space-charge-shifted frequencies. One such method involves the use of two lasers (optical-optical double resonance) and is relatively complicated [12]. However, it has the advantage of being more general in that much larger rotation frequencies of the ion cloud can be reached. The limitation of our method is that as the ion cloud contracts the degree of modulation decreases, making it increasingly difficult to measure the rotation frequency. Another method is to measure the frequencies of sidebands of an internal microwave resonance of the ions [13–15].

B. The contact potential

Although, in principle, the Penning trap remains stable down to arbitrarily small values of V_{dc}, we found we were unable to use the trap at voltages smaller than ~1.4 V. We find that as V_{dc} is lowered, we need to readjust radially the position of the cooling beam's focal spot to maintain the maximum fluorescence level. We infer that the effective center of the trap moves as a function of applied voltage.

We interpret this effect as being due to the presence of a contact potential: part of the copper ring electrode in our trap is coated by excess Mg atoms emanating from the oven. This sets up a contact potential of 0.91 V, which means that if we apply a potential of 0 V to the ring, the coated portion settles at a potential of 0.91 V. Furthermore, the extent of the coated region changes progressively with time as the oven is used. Some of the effects of such contact potentials have been noted by other authors (e.g., Ref. [7]).

For a Penning trap, the effective trap center always occurs at the position of the saddle point in the electrostatic potential, where there is a potential maximum in the radial plane. This is true even if, due to some distortion of the potential, the position of the saddle point does not coincide with the geometrical center of the trap (in an ideal trap the saddle point always occurs at the geometrical center of the trap). The inclusion of a contact potential creates such a distortion of the electric field and so shifts the effective trap center. Since our observations suggest that the effective trap center moves in the up-down direction as a function of V_{dc}, we approximate this distortion as a linear potential in the x direction set up by an area of contact potential at the position where the electrodes are coated with magnesium. The linear approximation should be quite good for small displacements from the geometrical trap center.

The quadrupole potential created by the application of V_{dc} to the electrodes is given by

$$V(\mathbf{r}) = V_{dc}\left[\frac{1}{2} + \frac{(2z^2 - r^2)}{R^2}\right], \tag{5}$$

where we have adopted the convention that the zero of voltage is the potential applied to the ring electrode. For the Penning trap with the inclusion of the contact potential, we model the radial potential in the up-down (x) direction close to the trap center as

$$V_x = V_{dc}\left[\frac{1}{2} - \frac{x^2}{4z_0^2}\right] + V_c\left[\frac{1}{2} - \frac{x}{2x_0}\right], \tag{6}$$

where V_c is the effective contact potential, $2x_0$ is the inner diameter of the ring electrode ($x_0 \equiv r_0$), and the $+x$ direction is defined to be up. In Fig. 5 we plot the resultant potential when the quadratic term contributed by the quadrupole potential is added to the linear contribution of the contact potential. This is done for a range of values of V_{dc}. The progressive shift of the maximum in the potential as V_{dc} is lowered is clearly demonstrated.

However, the unusual situation in the Penning trap, in which the ions move around a radial potential hill rather than being confined to a potential well leads to some surprising behavior when a field distortion is included. One would normally expect a spot of positive contact potential to *repel* the ion cloud, but Fig. 5 shows that the saddle point actually moves *towards* the coated portion.

The more usual situation, in which the ions reside at the bottom of a potential well, occurs in the Paul trap. If a positive contact potential is introduced in this type of trap, the ion will move up the side of the potential well to a position where the force of the confining potential cancels the force exerted by the contact potential. In this case the ion will indeed move *away* from the coated electrode, as expected. In the Penning trap, upon the imposition of a positive contact potential, the ion will still move on the confining potential surface to a position where the forces on it cancel. However, now this confining potential is a hill and for this unusual situation the position of zero resultant force occurs *closer* to the coated portion of the electrode.

This behavior is only in accordance with our obser-

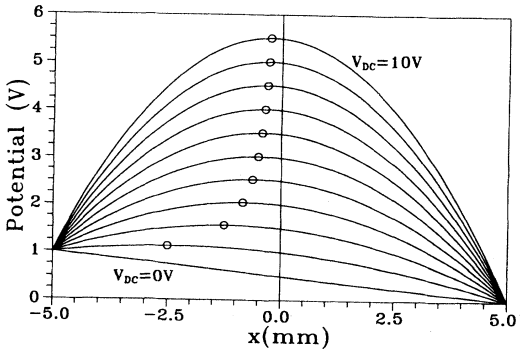

FIG. 5. Composite potential that results from adding a linear term, modeling the effect of the contact potential, to the quadratic term of the usual trapping potential. The resultant potential is drawn for 11 different values of V_{dc} with $V_c = 1$ V. The locus of the maximum in the potential (circles) shows how the effective center of the trap moves as a function of V_{dc}.

vations (that the ion cloud moves downwards as V_{dc} is lowered) if we assume that the coated portion of the ring electrode is below the geometrical center of the trap. This cannot be checked without demounting the trap, but it accords with the position of the oven shown in Fig. 1. The Mg atoms can be expected to effuse from the oven nearly isotropically. The intensity of the atomic beam will drop off approximately as the inverse of the square of the distance from the source. Since the pinhole in the oven is situated near to the lower edge of the ring and one end cap, the greatest deposit should occur at these positions. This interpretation is consistent with the behavior of the trap when operated in the combined mode [16].

The effective contact potential [V_c in Eq. (6)] has an upper bound of 0.91 V (which is the actual contact potential). This effective potential is a complicated function of the position and distribution of the magnesium coating on the copper-ring electrode. Furthermore, we are only sensitive to the x displacement, so that we only see the effect of the projection of the full contact potential onto the x axis.

The position of the maximum of the composite potential of Eq. (6) is given by

$$x_{\max} = -\frac{z_0^2 V_c}{V_{dc} x_0}. \tag{7}$$

We have measured the position of the effective trap center as a function of applied dc voltage for the Penning trap (see Fig. 6). This is done by calibrating the micrometer that tilts the laser input mirror. This gives a shift of the laser focal spot at the center of the trap of 25 μm per micrometer division. We have defined the zero of the x coordinate to be at the position of our first data point at 9 V. However, the effective trap center only asymptotically approaches coincidence with the geometrical trap center as V_{dc} is increased. We cannot therefore fit our data directly to Eq. (7) but must allow for an offset x_1 and fit our measured values of the position of the effective trap center (x_{meas}) to the form

$$x_{meas} = x_{max} + x_1. \tag{8}$$

Taking the values $z_0 = 3.5$ mm and $x_0 = 5.0$ mm for our trap, a least-squares fit of x_{max} to the form given by Eqs. (7) and (8) gives a value of 0.38 V for V_c, the effective contact potential for the geometry of our trap.

Operation of ideal (i.e., clean), hyperbolic electrodes in conjunction with the correct applied voltage and magnetic field, results in a stable Penning trap even down to voltages that are arbitrarily close to zero. It is interesting that the same arrangement, but with the inclusion of a contact potential, does not in fact result in a trap if the voltage is below a certain value. This lower bound to the voltage is given by setting $x_{max} = x_0$. As V_{dc} is lowered, this is the voltage at which the effective trap center coincides with the ring electrode. For our trap this gives a lower limit of 0.19 V. A more practical limit in our trap is realized long before this voltage is reached at around 1.4 V, when the ion cloud has moved out of the window created by the access holes in the ring electrode. Beyond this voltage, laser cooling and fluorescence detection cannot be performed.

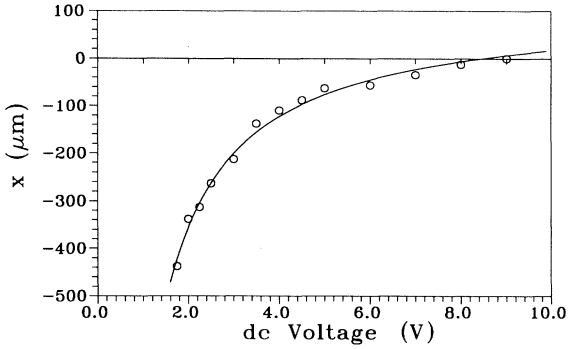

FIG. 6. Experimentally measured position of the effective center of the trap as a function of V_{dc}. The solid line is a fit to the form of Eq. 8.

C. Penning trap ion-oscillation frequencies

Values of $r_0 = 5.0$ mm and $z_0 = 3.5$ mm were set for our trap at the design stage. The ring and two end-cap electrodes are all machined out of oxygen-free copper and are then assembled on a chassis of alumina rods. The actual value of r_0 realized should be quite close to 5.0 mm since the ring electrode is machined out of a single piece of copper. However, given our method of construction, it is not possible to ensure the end-cap separation $2z_0$ is set at exactly the desired value. As a result we treat R^2 as a parameter to be measured by experiment. Equation (2) shows that a plot of ω_z^2 against V_{dc} gives a straight line with the gradient given by $4e/MR^2$. We have measured ω_z as a function of V_{dc} for a Penning trap, using our photon-photon correlation method. Figure 7 is the resulting plot of $\nu_z^2[= (\omega_z/2\pi)^2]$ against V_{dc}. The fact that this graph does not pass through the origin is another consequence of the contact potential.

The solid line is a linear fit to the data points above V_{dc}=5 V. The fitting procedure gives an intercept on the V_{dc} axis of 0.245 V, with the gradient giving R^2=5.44×10^{-5} m^2. Although the intercept on the V_{dc} axis is related to the presence of the contact potential, its value is not a measure of V_c as defined in the previous

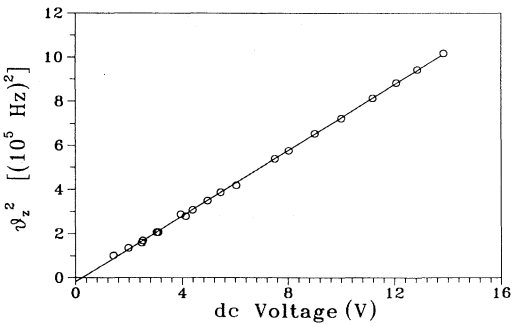

FIG. 7. Plot of ν_z^2 against V_{dc} for the Penning trap.

section. We used our composite potential to explain the shift in the position of the effective trap center. However, the value of ω_z depends on the curvature of the potential, rather than upon the position of the saddle point. For the model composite potential we have used, the curvature is not affected by the addition of the linear term (the curvature in the x direction *is* related to the curvature in the z direction through Poisson's equation). Therefore, to explain the change in ω_z which results from the contact potential we would need to include nonlinear terms in a full three-dimensional model potential.

We have used the new value of R^2 in Eqs. (1)–(4) to calculate theoretical values for the magnetron and modified cyclotron frequencies as a function of $V_{\rm dc}$. In this calculation we have included an offset in $V_{\rm dc}$ of 0.25 V to take into account the effect of the contact potential. Using a Hall probe, we have measured the magnetic field B to be 0.98 $\pm$0.01 T. In order to make this measurement, it was necessary to remove the trap from the space between the pole pieces. Insertion of the trap into the gap may perturb the magnetic field by a small amount. To achieve a fit to our measured values for ω_c' and ω_m we have allowed B to vary slightly. We have adopted the procedure of fitting the modified cyclotron data in this way, and then using the resulting value of $B = 0.94$ T to calculate the theoretical magnetron frequency curve. Given that the frequencies differ by a factor of 5–10 the resulting agreement for the magnetron data is very good (see Fig. 8).

In Fig. 8 the scatter in the modified cyclotron data is greater than the scatter in the magnetron data. This is probably due to slight variations in the unstabilized magnetic field. The magnetron and modified cyclotron frequencies depend approximately inversely and linearly on the magnetic field, respectively. For the magnetron frequency a small percentage change in B will go unnoticed but for the much larger modified cyclotron frequency, a 1% change in B gives a shift of $\sim$5 kHz. The axial frequency is entirely independent of the magnetic field leading to the excellent fit in Fig. 7.

We have found that the modified cyclotron modulation is usually at its greatest immediately after loading the trap. As the ion cloud cools, this modulation usually decreases, leaving the magnetron modulation dominating the correlation plot. Consequently, it is more difficult to obtain data for the modified cyclotron frequency. We have tried unsuccessfully to "reheat" the ion cloud in a number of ways, to retrieve the modified cyclotron modulation. For example, we have tried temporarily tuning the laser above rather than below the cooling transition. We have not found this to have the desired effect. We have also tried driving the cloud temporarily at $V_{\rm ac}$. When this is done, the modified cyclotron modulation reappears but quickly disappears again as soon as the drive is turned off. We also note that data for the modified cyclotron frequency is more difficult to obtain at higher values of $V_{\rm dc}$. In this situation the axial potential well becomes deeper, forcing the ions toward the radial plane. In this regime we find our correlation plots to be dominated by the magnetron and axial frequencies and their harmonics. Preliminary results from a computer simulation program we are presently developing confirm that the laser cooling preferentially reduces the cyclotron motion in this regime.

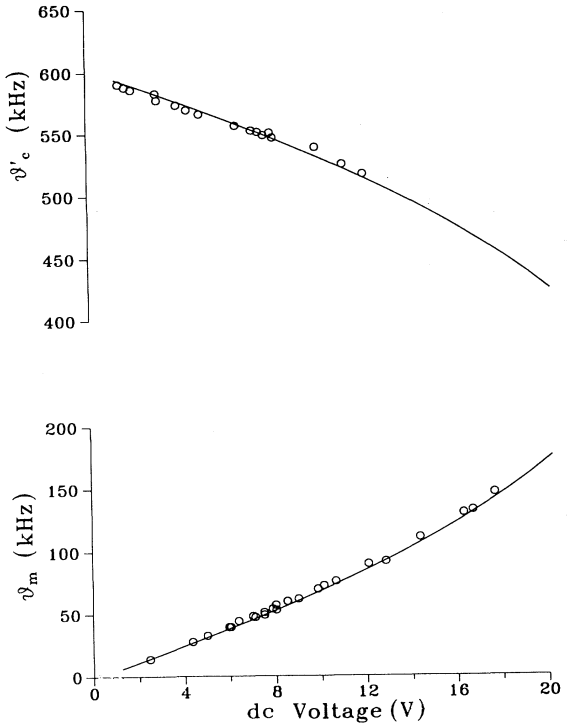

FIG. 8. Plot of the magnetron and modified cyclotron frequencies as a function of $V_{\rm dc}$. The modified cyclotron data are fitted using the parameters determined from Fig. 7 and a variable magnetic-field parameter. The magnetron curve has no free parameters.

IV. CONCLUSIONS

We have demonstrated a simple and effective method for measuring ion-oscillation frequencies in quadrupole ion traps. We have used the method to verify the ion-oscillation frequencies of the Penning trap over a large range of the applied dc voltage. We have shown that, as expected, our method measures space-charge-shifted oscillation frequencies. We have discussed the shift in the position of the effective center of the trap caused by the presence of the contact potential. In future work we intend to use the method to study the possible formation of crystals of small numbers of ions in a Penning trap, such as those seen in Paul traps. Such crystals could not be imaged in a Penning trap due to the inherent rotation of the ions at the magnetron frequency. Crystallization should be accompanied by the appearance of new characteristic frequencies in the photon-photon correlation spectrum.

ACKNOWLEDGMENTS

We gratefully acknowledge the support of the U.K. Science and Engineering Research Council. One of us (G.Zs.K.H.) would like to thank the Swiss National Science Foundation and the Royal Society for financial support.

* Permanent address: Department of Physics, University of Otago, Dunedin, New Zealand.

[1] See, e.g., R. Blatt, P. Gill, and R.C. Thompson, J. Mod. Opt. **39**, 193 (1992).
[2] E. Fischer, Z. Phys. **156**, 1 (1959).
[3] L.S. Brown and G. Gabrielse, Rev. Mod. Phys. **58**, 233 (1986).
[4] D.J. Bate, K. Dholakia, R.C. Thompson, and D.C. Wilson, J. Mod. Opt. **39**, 305 (1992).
[5] D.J. Wineland, W.M. Itano, and R.S. Van Dyck, Jr., Adv. At. Mol. Phys. **19**, 135 (1984).
[6] F. Diedrich, E. Peik, J.M. Chen, W. Quint, and H. Walther, Phys. Rev. Lett. **59**, 2931 (1987); D.J. Wineland, J.C. Bergquist, W.M. Itano, J.J. Bollinger, and C.H. Manney, *ibid.* **59**, 2935 (1987); R. Blümel, J.M. Chen, E. Peik, W. Quint, W. Schleich, Y.R. Shen, and H. Walther, Nature **334**, 309 (1988).
[7] R. Blümel, C. Kappler, W. Quint, and H. Walther, Phys. Rev. A **40**, 808 (1989).
[8] S.L. Gilbert, J.J. Bollinger, and D.J. Wineland, Phys. Rev. Lett. **60**, 2022 (1988).
[9] G-Z. Li, Comm. Theor. Phys. (China) **12**, 355 (1989).
[10] H. Imajo, S. Urabe, K. Hayasaka, and M. Watanabe, J. Mod. Opt. **39**, 317 (1992).
[11] F. Diedrich and H. Walther, Phys. Rev. Lett. **58**, 203 (1987).
[12] L.R. Brewer, J.D. Prestage, J.J. Bollinger, W.M. Itano, D.J. Larson, and D.J. Wineland, Phys. Rev. A **38**, 859 (1988).
[13] D.J. Heinzen, J.J. Bollinger, F.L. Moore, W.M. Itano, and D.J. Wineland, Phys. Rev. Lett. **66**, 2080 (1991).
[14] H.S. Lakkaraju and H.A. Schuessler, J. Appl. Phys. **53**, 3967 (1982).
[15] V. Enders, Ph. Courteille, W. Neuhauser, and R. Blatt, J. Mod. Opt. **39**, 325 (1992).
[16] K. Dholakia, D.M. Segal, G.Zs.K. Horvath, and R.C. Thompson, J. Mod. Opt. (to be published).